448-Gb/s Reduced-Guard-Interval CO-OFDM Transmission Over 2000 km of Ultra-Large-Area Fiber and Five 80-GHz-Grid ROADMs

Xiang Liu, *Senior Member, IEEE*, S. Chandrasekhar, *Fellow, IEEE*, Benyuan Zhu, *Member, IEEE*, P. J. Winzer, *Fellow, IEEE*, Alan H. Gnauck, *Fellow, IEEE*, and David W. Peckham, *Senior Member, IEEE*

***Abstract*—We propose a novel coherent optical orthogonal frequency-division multiplexing (CO-OFDM) scheme with reduced guard interval (RGI) for high-speed high-spectral-efficiency long-haul optical transmission. In this scheme, fiber chromatic dispersion is compensated for within the receiver rather than being accommodated by the guard interval (GI) as in conventional CO-OFDM, thereby reducing the needed GI, especially when fiber dispersion is large. We demonstrate the generation of a 448-Gb/s RGI-CO-OFDM signal with 16-QAM subcarrier modulation through orthogonal band multiplexing. This signal occupies an optical bandwidth of 60 GHz, and is transmitted over 2000 km of ultra-large-area fiber (ULAF) with five passes through an 80-GHz-grid wavelength-selective switch. Banded digital coherent detection with two detection bands is used to receive this 448-Gb/s signal. Wavelength-division multiplexed transmission of three 80-GHz spaced 448-Gb/s RGI-CO-OFDM channels is also demonstrated, achieving a net system spectral efficiency of 5.2 b/s/Hz and a transmission distance of 1600 km of ULAF.**

***Index Terms*—Coherent optical orthogonal frequency-division multiplexing (CO-OFDM), polarization-division multiplexing (PDM), wavelength-division multiplexing (WDM).**

I. Introduction

HIGH-SPEED optical transmission with per-channel data rates beyond 100 Gb/s is being actively researched for future optical transport systems [1]–[6], with 400-Gb/s Ethernet (400GbE) being a likely next step [7], [8]. To increase the overall system capacity, it is important to achieve high spectral efficiency (SE) when scaling up the wavelength-division multiplexed (WDM) per-channel bit rate. This can be achieved by imposing higher-order modulation on a single optical carrier for single-carrier transmission, or on multiple carriers for multi-carrier transmission [3]–[6]. Independent of the approach taken, the SE is defined as the ratio of the net bit rate per WDM channel to the WDM channel spacing. In multi-carrier formats such as coherent optical orthogonal frequency-division multiplexing (CO-OFDM), each WDM channel is composed of multiple optical subcarriers, and one can define an intra-channel SE (iSE) [4], [5] as the ratio of the net bit rate per subcarrier to the subcarrier spacing. The iSE constitutes an upper bound on the SE achievable in WDM operation, i.e., $\mathrm{iSE} \geq \mathrm{SE}$. Using multi-band CO-OFDM with polarization-division-multiplexed (PDM) quadrature phase-shift keying (QPSK) for subcarrier modulation, channel data rates of about 1 Tb/s have been demonstrated at an iSE ranging from 3.1 to 3.3 b/s/Hz [4], [5]. Using no-guard-interval (NGI) CO-OFDM [6], a 1.2-Tb/s signal based on PDM-QPSK was transmitted over 7200 km of ultra-large-area fiber (ULAF) at an iSE of 3.7 b/s/Hz [9]. Recently, optical transmission at higher SE has been demonstrated using 16-QAM [10], 32-QAM [11], and 36-QAM [12], respectively achieving SEs of 6.2 b/s/Hz at 112 Gb/s over 630 km, 7 b/s/Hz at 65 Gb/s over 240 km, and 8 b/s/Hz at 107 Gb/s over 320 km. More recently, 64-QAM was used to realize a per-channel bit rate of 240 Gb/s [13], but significant error floors were observed and its long-haul transmission has not been demonstrated. For optical backbone transport systems, it is desirable to achieve high SE at high per-channel data rate while maintaining long-haul transmission capability. We recently reported the generation and detection of a novel spectrally-efficient format, reduced-guard-interval (RGI) CO-OFDM, at 448 Gb/s with an iSE of 7 b/s/Hz, and transmitted this signal over 2000 km of ULAF with five passes through an 80-GHz-grid wavelength-selective switch (WSS) [14]. This demonstration represented the longest transmission distance for >200-Gb/s transmission within an optical bandwidth allowing for WDM transmission at SEs higher than 4 b/s/Hz., the first 400-Gb/s transmission over 2000 km, and the lowest overhead (7.3%) for >100-Gb/s CO-OFDM transmission with ≥40000-ps/nm accumulated CD.

In this paper, we describe in more detail the concept of RGI-CO-OFDM and the single-channel 448-Gb/s transmission experiment reported in [14]. In addition, more recent results on wavelength-division-multiplexed (WDM) transmission with three 448-Gb/s RGI-CO-OFDM channels will be presented. This paper is organized as follows. We first describe the concept of RGI-CO-OFDM and its pros and cons as compared to the conventional CO-OFDM in Section 2. We then detail the experimental results obtained on single-channel 448-Gb/s RGI-CO-OFDM transmission in Section 3. Section 4 presents the WDM transmission of three 80-GHz-spaced 448-Gb/s

Manuscript received June 10, 2010; revised September 16, 2010; accepted September 16, 2010. Date of publication October 07, 2010; date of current version February 02, 2011. This work was supported in part by the IT R&D Program of MKE/KEIT (2008-S-044-1), Korea.

X. Liu, S. Chandrasekhar, P. J. Winzer, and A. H. Gnauck are with Bell Labs, Alcatel-Lucent, Holmdel, NJ 07733 USA (e-mail: xiang.liu@alcatel-lucent.com).

B. Zhu and D. W. Peckham are with OFS Labs, Somerset, NJ 08873 USA.

Color versions of one or more of the figures in this paper are available online at http://ieeexplore.ieee.org.

Digital Object Identifier 10.1109/JLT.2010.2084988

RGI-CO-OFDM channels, achieving a net system SE of 5 b/s/Hz and a transmission distance of 1600 km. Finally, Section 5 concludes this paper.

II. Concept of RGI-CO-OFDM

In conventional CO-OFDM, a guard interval (GI), e.g., in the form of cyclic prefix (CP), is inserted in the time domain between adjacent OFDM symbols to accommodate fiber chromatic dispersion (CD) induced inter-symbol interference (ISI) [15]–[17]. For high-speed long-haul optical fiber transmission without inline optical dispersion compensation, the CD-induced channel memory length can be very large, so a large GI is required. The use of a larger GI leads to a larger unwanted temporal overhead, which results in substantial reduction of the SE, when the OFDM symbol size is fixed. On the other hand, when the OFDM symbol size is proportionally increased to maintain a fixed GI overhead, the subcarrier spacing, which scales as the inverse of the OFDM symbol size, decreases, resulting in tighter requirements on the optical frequency locking between the transmit laser and the receiver optical local oscillator (OLO). The technical problem that our work aims to solve is how to enable high-speed (e.g., >100-Gb/s) CO-OFDM to be highly spectrally efficient and tolerant to the frequency offset between the OLO and the transmit laser in the presence of large fiber dispersion.

One solution to this problem is to completely remove the GI and rely on blind equalization at the receiver to compensate for fiber dispersion, as demonstrated in recent NGI-CO-OFDM experiments [6], [9]. However, without the GI, the ISI due to transmitter bandwidth limitations is not accommodated for, and more complex blind equalization is needed to compensate for the effect of polarization-mode dispersion (PMD) [17].

In the proposed RGI-CO-OFDM scheme [14], a reduced GI or CP between adjacent OFDM symbols is used to accommodate the ISI with *short memory*, such as induced by transmitter bandwidth limitations or fiber PMD, while fiber CD-induced ISI with *long memory* and *well-defined* characteristics is compensated at the receiver, as is done in single-carrier frequency-domain equalization (SC-FDE) systems [18]. In essence, RGI-CO-OFDM is a *hybrid* version of conventional CO-OFDM with CP and SC-FDE. Fig. 1 shows the schematic of the digital signal processing (DSP) structure of RGI-CO-OFDM. RGI-CO-OFDM shares most of the DSP modules used in conventional CO-OFDM, and the only new DSP modules used in RGI-CO-OFDM are those associated with receiver-side electronic dispersion compensation (EDC) based on discrete Fourier transform (DFT), inverse DFT (IDFT), and overlap-add [18]. The size of the M-point DFT and IDFT used for EDC is usually a few times the CD-induced channel memory length [18]. As the residual channel memory length is much shortened after the EDC, the GI length and the OFDM symbol size in RGI-CO-OFDM can be much shorter compared to conventional CO-OFDM. Using the 112-Gb/s PDM-OFDM design described in [19] as an example, the sampling rate of digital-to-analog converter (DAC) and analog-to-digital converter (ADC), $R_{DAC(ADC)}$, was assumed to be 56 GSamples/s, and the size of N-point DFT(IDFT) used, $N_{DFT(IDFT)}$, was 2048. The GI length in units of DAC sampling period, N_{GI}, was selected to be 512 in order to be longer than the CD-induced channel memory length in a dispersion-uncompensated transmission over 1500-km standard single-mode fiber ($D = 17$ ps/nm/km), which was ~500 samples. The GI-induced overhead, denoted as O_{GI}, is

$$O_{GI} = N_{GI}/N_{DFT(IDFT)}.$$

The overhead due to GI was thus 25% $(= 512/2048)$, which not only reduces the achievable SE but also causes an optical signal-to-noise-ratio (OSNR) penalty of ~1.8 dB. In RGI-CO-OFDM, the GI only needs to be longer than the memory length associated with PMD. With a GI length of 4 samples, 4/(56 GSamples/s) $= 71.4$ ps of instantaneous differential group delay (DGD) can be accommodated, which is sufficient for most of optical fiber transport systems. $N_{DFT/IDFT}$ can be shortened by a factor of 16, i.e., from 2048 to 128. As a result, the overhead and OSNR penalty due to the GI are dramatically reduced to 3.13% and 0.13 dB, respectively. The OFDM subcarrier spacing, Δf_{sc}, is related to $N_{DFT(IDFT)}$ as

$$\Delta f_{sc} = R_{DAC(ADC)}/N_{DFT(IDFT)}$$

so, a smaller $N_{DFT(IDFT)}$ also results in a larger subcarrier spacing, which is beneficial in relaxing the requirements on the optical frequency locking between the transmitter laser and the receiver OLO. Table I compares the overhead and laser stability requirements between the proposed RGI-CO-OFDM and the conventional CO-OFDM for dispersion-uncompensated standard single-mode fiber (SSMF) transmission. The laser stability requirement is characterized as the maximum allowable frequency offset between the OLO and the transmitter laser, $|\Delta f_{max}|$, which is conventionally defined as half of the OFDM subcarrier spacing, or $\Delta f_{sc}/2$.

Clearly, RGI-CO-OFDM offers much reduced overhead and relaxed laser stability requirements, independent of CD, in high-speed long-haul dispersion-uncompensated transmission. In practical systems, it is very difficult to control the frequency offset to be less than 30 MHz, as the typical frequency stability of a narrow-linewidth external-cavity laser is about ± 300 MHz over a period of 24 hours even when the laser temperature is stabilized to a given value within $\pm 0.5°$C [20]. At data rates higher than 112 Gb/s, the CD-induced memory length can be even longer, and the benefits of RGI-CO-OFDM are expected to be more pronounced.

With the shortened GI and OFDM symbol size, there are several additional benefits: (1) shorter training symbols (TSs), leading to a lower TS-induced overhead and a lower computational load for channel synchronization, frequency estimation, and channel estimation, (2) shorter OFDM frames, leading to higher channel tracking speed and higher tolerance to clock or sampling frequency offset between the transmitter DAC and the receiver ADC, and (3) a higher tolerance to laser linewidth. The only expense we have to pay when applying RGI-CO-OFDM is the use of additional DSP to perform EDC before OFDM de-multiplexing at the receiver. Nevertheless, owing to the DSP efficiency of OFDM [17], the overall DSP complexity of RGI-CO-OFDM is expected to be lower or similar to that of SC-FDE.

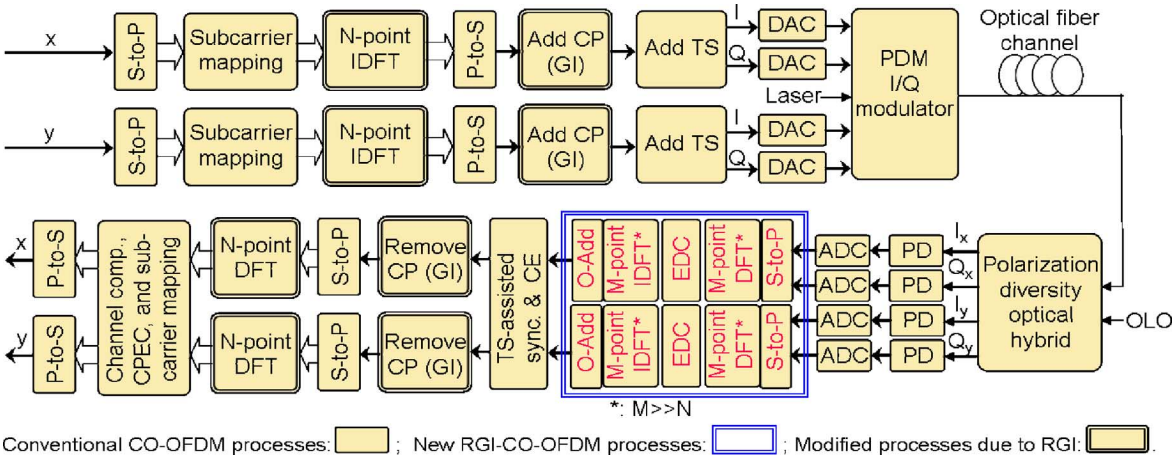

Fig. 1. Schematic of the DSP structure of RGI-CO-OFDM with PDM. S-to-P: Serial-to-Parallel; (I)DFT: (inverse) discrete Fourier transform; P-to-S: parallel-to-serial; TS: training symbol; DAC: digital-to-analog convertor; ADC: analog-to-digital convertor; PD: photo-diode; EDC: electronic dispersion compensation; O-Add: overlap-add; CE: channel estimation; CPEC: common phase error correction; OLO: optical local oscillator.

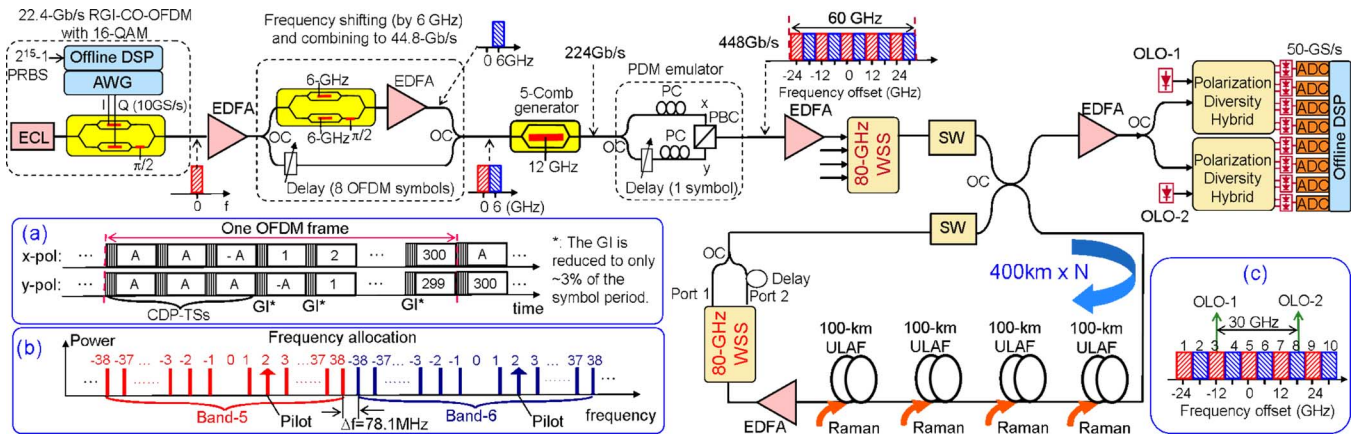

Fig. 2. Schematic of the single-channel transmission experimental setup. Insets: (a) OFDM frame arrangement; (b) Frequency allocation of the OFDM subcarriers; and (c) Configuration of the banded digital coherent detection with 2 OLOs. OC: optical coupler; PC: polarization controller; EDFA: Erbium-doped fiber amplifier; SW: optical switch.

TABLE I
COMPARISON BETWEEN CONVENTIONAL CO-OFDM AND RGI-CO-OFDM FOR 112-GB/S TRANSMISSION WITH $R_{DAC(ADC)} = 56$ GSSAMPLE/S

System Reach	Conventional CO-OFDM (N_{GI} is CD dependent)		RGI-CO-OFDM (N_{GI}=4; N_{IDFT}=128)	
	O_{GI} (=N_{GI}/N_{IDFT})	$\lvert\Delta f_{max}\rvert$	O_{GI}	$\lvert\Delta f_{max}\rvert$ (=$\Delta f_{sc}/2$)
1,500-km SSMF	25% (=512/2048)	13.7 MHz	3.13%	218 MHz
	50% (=512/1024)	27.3 MHz	3.13%	218 MHz
3,000-km SSMF	25% (=1024/4096)	6.8 MHz	3.13%	218 MHz
	50% (=1024/2048)	13.7 MHz	3.13%	218 MHz

III. SINGLE-CHANNEL 448-GB/S TRANSMISSION

A. Experimental Setup

Fig. 2 shows the schematic of the experimental setup for single-channel transmission [14]. At the transmitter, offline DSP was first performed to generate an OFDM waveform, which was then stored in an arbitrary waveform generator (AWG). In the offline DSP, a data stream consisting of a pseudo-random bit sequence (PRBS) of length $2^{15} - 1$ was mapped onto 75 16-QAM subcarriers, which, together with one pilot subcarrier, one unfilled (i.e., zero-power) DC subcarrier, and 51 unfilled edge subcarriers, was converted to the time domain via an IFFT of size 128. The filled subcarriers were pre-emphasized to mitigate transmitter bandwidth roll-off. A small GI of length 4 samples was used, resulting in an OFDM symbol size of 132. To facilitate OFDM frame synchronization and channel estimation, four training symbols (TSs), [A A A − A], where A is a known OFDM symbol, were inserted at the beginning of each OFDM frame that contained 300 data symbols. Note that after PDM (to be discussed later), there were three correlated dual-polarization (CDP) TSs, as shown in inset (a) of Fig. 2. The first two CDP-TSs were identical and used for autocorrelation-based frame synchronization, and the last two CDP-TSs were for channel estimation. The TS power was equal to the average data symbol power to mitigate some penalty from fiber nonlinearity [21]. Intra-symbol frequency-domain averaging [19] was later applied at the receiver to improve the accuracy of the channel estimation based on only two TSs. The real and imaginary parts of the OFDM waveform were clipped

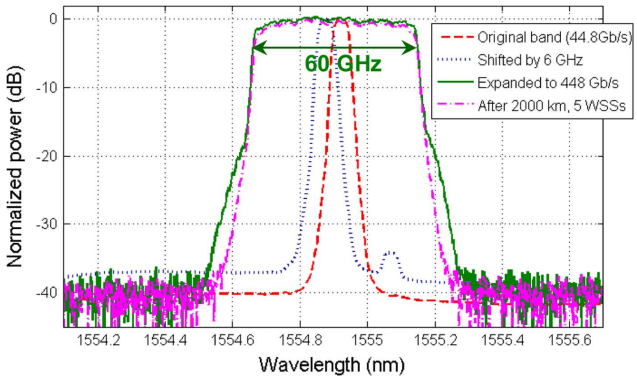

Fig. 3. Measured optical signal spectra at various stages.

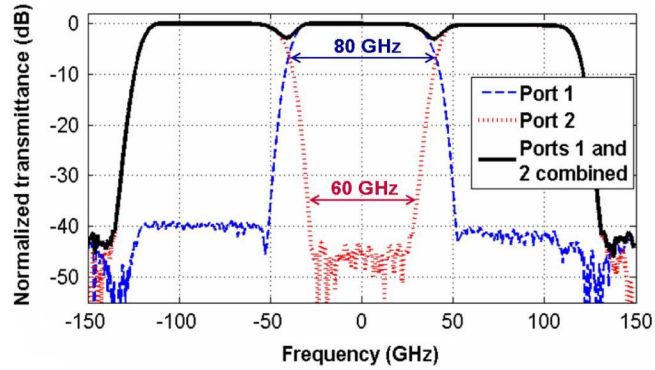

Fig. 4. Passband characteristics of the 80-GHz-grid WSS used in the loop.

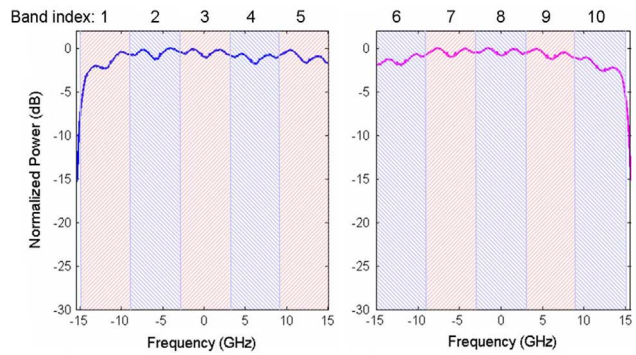

Fig. 5. RF spectra of the lower (left) and upper (right) halves of the 448-Gb/s signal, respectively covering the first and last five OFDM bands.

with a clipping ratio of 6 (the samples whose powers are more than 6 times of the mean sample power are set to 6) [19], and converted to analog waveforms by two DACs operating at 10 GS/s, which were amplified and used to drive an optical I/Q modulator connected to an external-cavity laser (ECL) with 100-kHz linewidth. A CO-OFDM signal at 22.4 Gb/s ($=$ 10Gb/s $\cdot 4 \cdot 75/132 \cdot 300/304$) with a spectral bandwidth of 6.016 GHz ($=$ 10 GHz $\cdot 77/128$) was thus formed. The signal was split into two copies, one being frequency shifted by exactly 6.016 GHz through a single-sideband modulator and the other being delayed by 8 OFDM symbol periods relative to the first copy, before being *seamlessly* recombined to form a 44.8-Gb/s signal consisting of two decorrelated bands, as illustrated in Fig. 2 and inset (b). The combined 2-band signal was expanded by a 5-comb generator based on an overdriven Mach–Zehnder modulator to form a 10-band 224-Gb/s signal. The above arrangement ensured that adjacent bands contained different data patterns (for de-correlation purposes) and produced minimal coherent crosstalk among the 10 bands. Note that in real implementations, 10 independent modulators would need to be used to form the 10-band RGI-CO-OFDM signal. Note also that by using higher speed DACs and modulators, the number of optically multiplexed bands can be reduced to simplify the optics. A PDM emulator (with one-symbol delay between the two polarizations) was used to double the data rate to generate a 448-Gb/s signal with a bandwidth of 60.16 GHz. Fig. 3 shows the measured optical spectra at various stages of the generation process. Notably, the total overhead due to OFDM in this RGI-CO-OFDM signal was only 7.3% and was independent of CD.

The signal was launched into a transmission loop [9], consisting of four Raman-amplified 100-km ULAF spans. The average fiber loss, dispersion, and dispersion slope at 1550 nm were 0.185 dB/km, 19.9 ps/nm/km, 0.06 ps/nm^2/km, respectively. The effective area was 120 μm^2. Span amplification was provided solely by backward Raman pumping. One erbium-doped fiber amplifier (EDFA) was used to compensate for the remaining loss in the loop. To evaluate the performance of the 448-Gb/s channel in optically routed networks with reconfigurable optical add/drop multiplexers (ROADMs), we used two flexible-bandwidth WSSs (Finisar WaveShaper 4000S) configured for 80-GHz channel spacing, one before and the other in the loop. Note that the unwanted sidebands generated by the 5-comb generator were filtered by the input WSS. To emulate the joint impact of filtering and inband crosstalk from non-ideal wavelength-blocking at ROADMs, we configured the WSS output port 1 to pass the signal and port 2 to block the signal, and combined the two ports before the signal went on for the next round trip. By doing so, the inband crosstalk due to the finite rejection ratio of the WSS is added to the original signal. The transmittances of the two ports are shown in Fig. 4. The 0.2-dB and 3-dB bandwidth of port 1 was 60 GHz and 80 GHz, respectively, and the rejection of crosstalk from port 2 in the signal bandwidth ($\pm$30 GHz) was $>$33 dB, from which we expect a small filtering and crosstalk penalty even after five WSS passes.

At the receiver, four asynchronously sampling 50-GS/s ADCs embedded in a real-time sampling oscilloscope with 16-GHz RF bandwidth were used. Due to the ADC bandwidth limitation, a banded digital coherent detection approach with 2 optical local oscillators (OLOs) had to be used to recover the entire 448-Gb/s signal, as shown in inset (c) of Fig. 2 In the experiment, we sequentially detected the lower (long-wavelength) and upper (short-wavelength) halves of the signal with one optical frontend by setting the OLO to -15 GHz and $+15$ GHz relative to the signal center frequency, respectively. Fig. 5 shows the RF spectra of the recovered two halves of the signal, respectively covering the first and last five OFDM bands as illustrated in Fig. 2. Exemplarily recovered subcarrier constellations are shown in Fig. 6. The digitized waveforms were stored and processed offline. Most of the DSP modules were similar to those described in [21]. The main new DSP module is the compensation of self-phase modulation (SPM) [22] and CD through a multi-step FFT-based algorithm, similar to that for single-carrier transmission [23], [24], where the number of steps equals

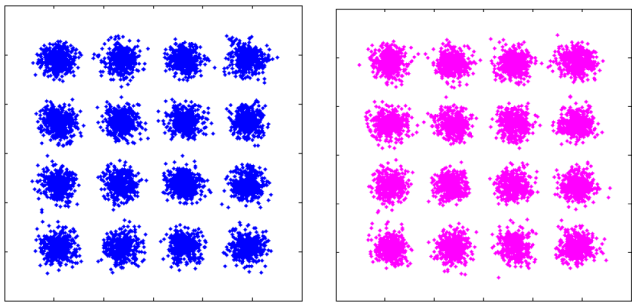

Fig. 6. Typical recovered subcarrier constellations in the lower (left) and upper (right) halves of the 448-Gb/s signal.

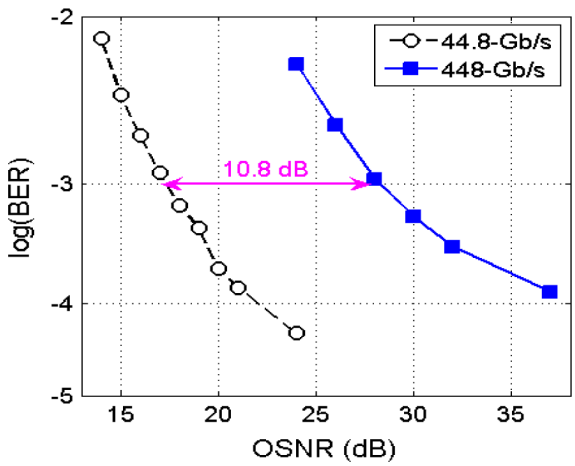

Fig. 7. Measured BER performance of the 10-band 448-Gb/s RGI-CO-OFDM signal as compared to the original single-band 44.8-Gb/s signal.

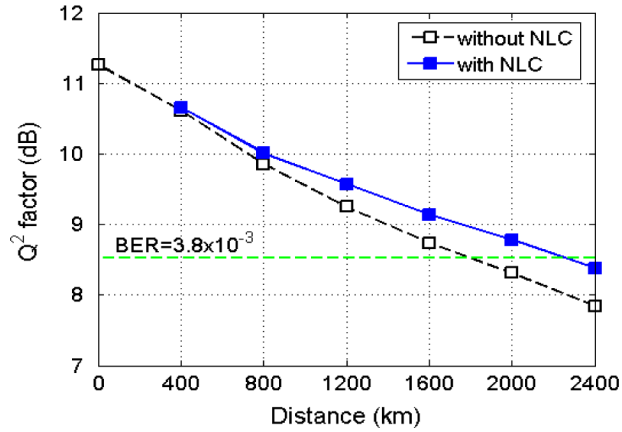

Fig. 8. Measured Q^2 factor as a function of transmission distance.

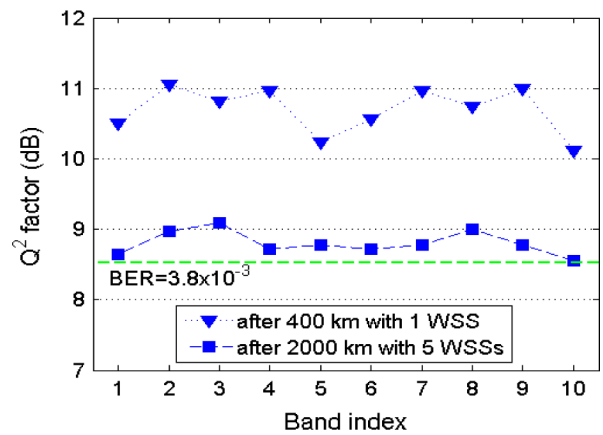

Fig. 9. Measured Q^2 factor versus band index.

the number of fiber spans. This receiver-side module for EDC and fiber nonlinearity compensation (NLC) not only reduces the OFDM overhead, but also improves the signal tolerance to fiber nonlinearity.

B. Experimental Results

Fig. 7 shows the measured bit error ratio (BER) as a function of OSNR (0.1-nm noise bandwidth; both noise polarizations). At $\mathrm{BER} = 1 \times 10^{-3}$, the required OSNR for the 448-Gb/s signal is 28.2 dB, which is 10.8 dB higher than that for the original single-band 44.8-Gb/s signal, showing a small excess penalty of ~0.8 dB due to band multiplexing and simultaneous detection of only 5 bands instead of the entire orthogonal multiplex per shot. At $\mathrm{BER} = 3.8 \times 10^{-3}$, the threshold of an advanced 7% FEC [25], [26], the required OSNR is ~25 dB, within 3.5 dB from the theoretical limit. For 2000-km transmission, the optimal signal launch power was found to be about 1.5 dBm, at which the OSNR after transmission was 28.5 dB. Fig. 8 shows the Q^2 factor, derived from the measured BER, as a function of transmission distance. With NLC, the mean BER of the 448-Gb/s signal is below 3×10^{-3} after 2000-km transmission and 5 WSS passes. The total transmission penalty is ~3 dB. The reach improvement by the NLC is ~25%. Fig. 9 shows the Q^2 factor as a function of the band index with the use of NLC. The OFDM bands at the edges of the two halves (1, 5, 6, and 10) perform slightly worse than the other bands, primarily due to the bandwidth limitation of the ADCs. Compared to that after 1 WSS pass, the performance of the two outmost bands (1 and 10) after 5 WSS passes shows negligible additional penalty compared to the two center bands (5 and 6), possibly due to the balancing between the small WSS filtering penalty at bands 1 and 10 and the slightly higher nonlinear penalty at bands 5 and 6.

IV. WDM Transmission

A. Experimental Setup

After studying the performance of a single 448-Gb/s RGI-CO-OFDM channel at an iSE of 6.9 b/s/Hz, we set up a WDM experiment to test its performance in a WDM network at a SE of 5.2 b/s/Hz (excluding the 7% FEC overhead). Fig. 10 shows the schematic of the experimental setup for WDM transmission. At the transmitter, the outputs of three 80-GHz spaced external-cavity lasers (ECLs), each having 100-kHz linewidth were combined by an optical coupler, before being modulated the same way as described in the previous section to form three 448-Gb/s RGI-CO-OFDM channels. Fig. 11 shows the measured optical spectra of the three WDM channels before and after transmission. Note that unwanted high-order sidebands were produced by the 5-comb generator that caused an artificial coherent crosstalk penalty, which will not be present in real implementations where the 5-comb generator is replaced with 5 independent modulators. The WDM channels were launched into the same transmission loop as described in the previous section. An 80-GHz-grid WSS was inserted in the loop to first separate the two edge channels from the center channel and

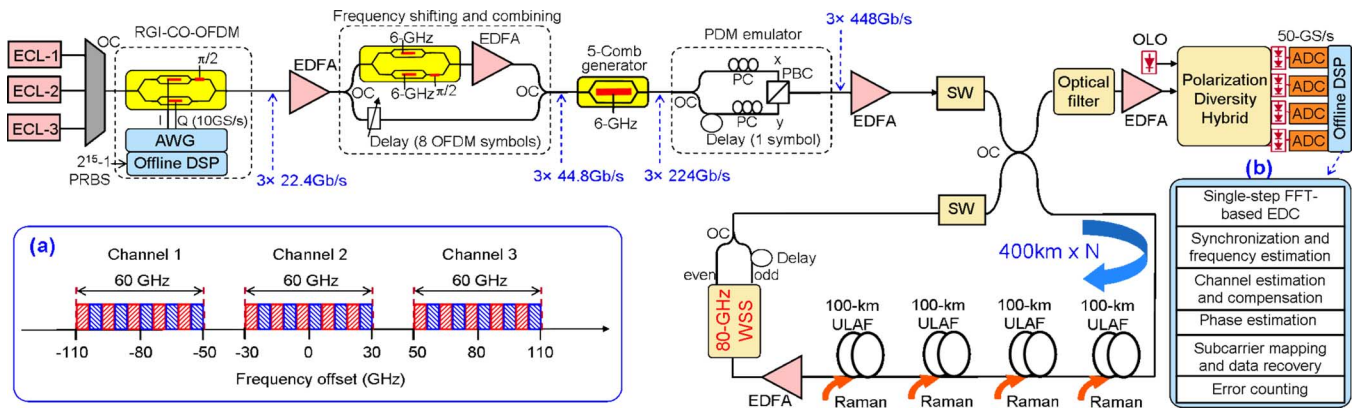

Fig. 10. Schematic of the experimental setup for WDM transmission. Insets: (a) WDM channel allocation; (b) Block diagram of the receiver DSP. OC: optical coupler; PC: polarization controller; PBC: polarization combiner; EDFA: Erbium-doped fiber amplifier; EDC: electronic dispersion compensation.

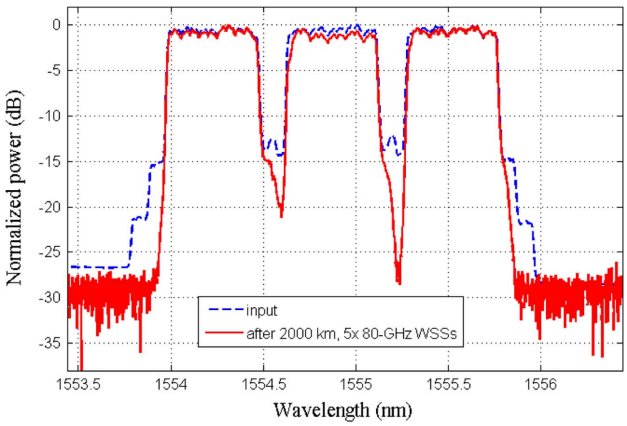

Fig. 11. Measured optical spectra of the three 80-GHz spaced 448-Gb/s RGI-CO-OFDM channels. Spectral resolution: 0.01 nm.

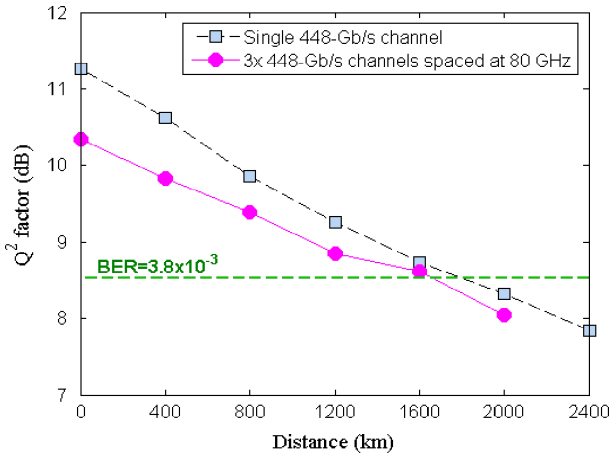

Fig. 12. Measured Q^2 factor of the center 448-Gb/s channel as a function of transmission distance. $P_{in} = 1.5$ dBm.

then combine them to emulate an optically routed link. At the receiver, each WDM channel was sequentially filtered out by a tunable optical filter with a 3-dB bandwidth of 100 GHz before detection. The receiver-side DSP blocks are shown in inset (b) of Fig. 10. To minimize the computational load, multi-step NLC was not performed. The fiber CD was compensated by a FDE-based EDC [18].

B. Experimental Results

Fig. 12 shows the BER of the center 448-Gb/s RGI-CO-OFDM channel as a function of transmission distance. For 1600-km transmission without NLC, the optimal signal launch power, P_{in}, was found to be about 1.5 dBm per channel. The mean BER of the center channel after 1600-km transmission and 4 WSS passes was 3.5×10^{-3}, below the threshold of a 7%-overhead FEC [25], [26]. Compared to the single-channel performance without NLC (also shown in Fig. 12), the WDM transmission performance is only slightly degraded, ~0.2 dB in Q^2 at 1600 km. Part of this degradation can be attributed to the OSNR degradation at the transmitter as three WDM channels share the same optical amplifiers. This can also be seen from the performance degradation at the back-to-back configuration (0 distance) shown in Fig. 12. It can thus be inferred that the inter-channel nonlinear penalty in the WDM transmission is small.

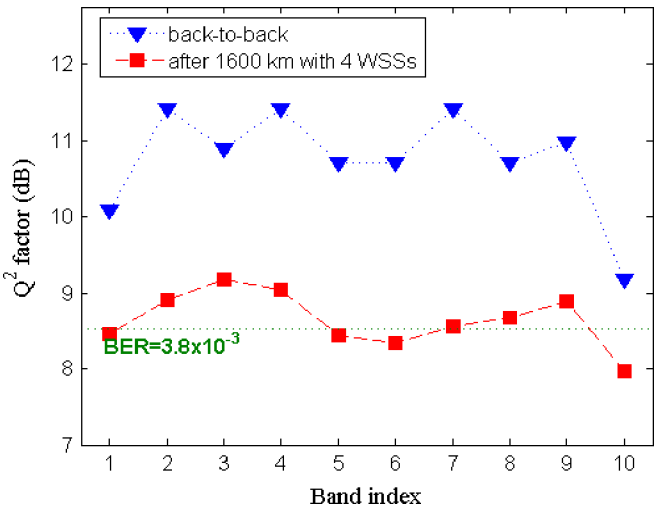

Fig. 13. Measured Q^2 factors of the 10 bands of the center channel versus band index before and after 1600-km transmission.

Fig. 13 shows the Q^2 factors of all the 10 bands of the center 448-Gb/s channel both before fiber transmission (back-to-back) and after 1600-km transmission at 1.5 dBm launch power per channel. The Q^2 factors of all the bands of the center channel

except for the two edge bands, are similar. We attribute the performance degradation of the edge bands to the linear coherent crosstalk artifact due to the unwanted sidebands produced by the 5-comb generator. After 1600-km transmission, the two center bands perform slightly worse than the average, possibly due to larger nonlinear penalty from neighboring bands in the same channel, as in the single-channel transmission case discussed in the previous section. Although the average BER over the 10 bands is below the FEC threshold, the BERs of bands 1, 5, 6, and 10 are slightly higher than the threshold, so it is needed to scramble (or interleave) all the bands of the 448-Gb/s channel in the FEC process.

V. Conclusion

We have proposed a novel RGI-CO-OFDM scheme aiming to take advantage of both CO-OFDM and SC-FDE and reduce the OFDM overhead to low values. We described the generation and detection of a 448-Gb/s RGI-CO-OFDM signal with 16-QAM subcarrier modulation, occupying a narrow optical bandwidth of 60 GHz. We transmitted the signal over 2000 (1600) km of 100-km low-loss low-nonlinearity ULAF spans and through five (four) 80-GHz-grid WSS-based ROADMs, achieving a BER below 3.8×10^{-3} with (without) the use of multi-step NLC. Furthermore, we have demonstrated the transmission of three 80-GHz-spaced 448-Gb/s RGI-CO-OFDM channels over 1600 km of 100-km ULAF spans and through four 80-GHz-grid WSS-based ROADMs with small WDM penalty, realizing a net system SE of 5.2 b/s/Hz. As a comparison, WDM transmission of seven 224-Gb/s RGI-CO-OFDM channels on a standard 50-GHz channel grid, achieving a net SE of 4.2 b/s/Hz, was recently demonstrated over 2000 km of ULAF without the NLC [27]. This shows the feasibility of realizing future high-SE long-haul 400GbE or 200GbE optical transport by using RGI-CO-OFDM.

Acknowledgment

The authors wish to thank A. R. Chraplyvy, R. W. Tkach, D. J. DiGiovanni, and R. L. Lingle, Jr. for support.

References

[1] A. R. Chraplyvy, "The coming capacity crunch," presented at the ECOC Plenary Talk, 2009.
[2] R. W. Tkach, "Scaling optical communications for the next decade and beyond," *Bell Labs Tech. J.*, vol. 14, pp. 3–10, 2010.
[3] A. D. Ellis, F. C. G. Gunning, B. Cuenot, T. C. Healy, and E. Pincemin, "Towards 1TbE using coherent WDM," in *Proc. OECC/ACOFT 2008*, Sydney, Australia, 2008, Paper WeA-1.
[4] Y. Ma, Q. Yang, Y. Tang, S. Chen, and W. Shieh, "1-Tb/s per channel coherent optical OFDM transmission with subwavelength bandwidth access," in *Proc. OFC'09*, Post-deadline paper PDPC1.
[5] R. Dischler and F. Buchali, "Transmission of 1.2 Tb/s continuous waveband PDM-OFDM-FDM signal with spectral efficiency of 3.3 bit/s/Hz over 400 km of SSMF," in *Proc. OFC'09*, Post-deadline paper PDP2.
[6] A. Sano, E. Yamada, H. Masuda, E. Yamazaki, T. Kobayashi, E. Yoshida, Y. Miyamoto, R. Kudo, K. Ishihara, and Y. Takatori, "No-guard-interval coherent optical OFDM for 100-Gb/s long-haul WDM transmission," *J. Lightw. Technol.*, vol. 27, no. 16, pp. 3705–3713, Aug. 2009.
[7] J. D'Ambrosia, "100 gagabit ethernet and beyond," *IEEE Commun. Mag.*, vol. 48, no. 3, pp. S6–S13, 2010.
[8] P. J. Winzer, "Beyond 100G ethernet," *IEEE Commun. Mag.*, vol. 48, no. 7, pp. 26–30, 2010.
[9] S. Chandrasekhar, X. Liu, B. Zhu, and D. W. Peckham, "Transmission of a 1.2-Tb/s 24-carrier no-guard-interval coherent OFDM superchannel over 7200-km of ultra-large-area fiber," in *Proc. ECOC'09*, Post-deadline paper PD2.6.
[10] A. H. Gnauck, P. J. Winzer, C. R. Doerr, and L. L. Buhl, "10×112-Gb/s PDM 16-QAM transmission over 630 km of fiber with 6.2-b/s/Hz spectral efficiency," in *Proc. OFC'09*, Post-deadline paper PDPB8.
[11] H. Takahashi *et al.*, "DWDM transmission with 7.0-bit/s/Hz spectral efficiency using 8×65.1-Gb/s coherent PDM-OFDM signals," in *Proc. OFC'09*, Post-deadline paper PDPB7.
[12] X. Zhou, J. Yu, M.-F. Huang, Y. Shao, T. Wang, L. Nelson, P. Magill, M. Birk, P. I. Borel, D. W. Peckham, and R. Lingle, "64-Tb/s (640×107-Gb/s) PDM-36QAM transmission over 320 km using both pre- and post-transmission digital equalization," in *Proc. OFC'10*, Post-deadline paper PDPB9.
[13] A. Sano *et al.*, "240-Gb/s polarization-multiplexed 64-QAM modulation and blind detection using PLC-LN hybrid integrated modulator and digital coherent receiver," in *Proc. ECOC'09*, Post-deadline paper PD2.2.
[14] X. Liu, S. Chandrasekhar, B. Zhu, P. J. Winzer, A. H. Gnauck, and D. W. Peckham, "Transmission of a 448-Gb/s reduced-guard-interval CO-OFDM signal with a 60-GHz optical bandwidth over 2000 km of ULAF and five 80-GHz-grid ROADMs," in *Proc. OFC'10*, Post-deadline paper PDPC2.
[15] W. Shieh, H. Bao, and Y. Tang, "Coherent optical OFDM: Theory and design," *Opt. Exp.*, vol. 16, pp. 841–859, 2008.
[16] S. L. Jansen, I. Morita, T. C. Schenk, and H. Tanaka, "Long-haul transmission of 16×52.5 Gbits/s polarization-division- multiplexed OFDM enabled by MIMO processing (Invited)," *J. Opt. Netw.*, vol. 7, pp. 173–182, 2008.
[17] P. Poggiolini, A. Carena, V. Curri, and F. Forghieri, "Evaluation of the computational effort for chromatic dispersion compensation in coherent optical PM-OFDM and PM-QAM systems," *Opt. Exp.*, vol. 17, pp. 1385–1403, 2009.
[18] R. Kudo, T. Kobayashi, K. Ishihara, Y. Takatori, A. Sano, and Y. Miyamoto, "Coherent optical single carrier transmission using overlap frequency domain equalization for long-haul optical systems," *J. Lightw. Technol.*, vol. 27, no. 16, pp. 3721–3728, Aug. 2009.
[19] X. Liu and F. Buchali, "Intra-symbol frequency-domain averaging based channel estimation for coherent optical OFDM," *Opt. Exp.*, vol. 16, pp. 21944–21957, 2008.
[20] [Online]. Available: http://cp.literature.agilent.com/litweb/pdf/5990-5512EN.pdf
[21] X. Liu, F. Buchali, and R. W. Tkach, "Improving the nonlinear tolerance of polarization-division-multiplexed CO-OFDM in long-haul fiber transmission," *J. Lightw. Technol.*, vol. 27, no. 16, pp. 3632–3640, Aug. 2009.
[22] A. J. Lowery, "Fiber nonlinearity pre- and post-compensation for long-haul optical links using OFDM," *Opt. Exp.*, vol. 15, p. 12965, 2007.
[23] S. Oda, T. Tanimura, T. Hoshida, C. Ohshima, H. Nakashima, Z. Tao, and J. C. Rasmussen, "112 Gb/s DP-QPSK transmission using a novel nonlinear compensator in digital coherent receiver," in *Proc. OFC'09*, Paper OThR6.
[24] D. S. Millar, S. Makovejs, V. Mikhailov, R. I. Killey, P. Bayvel, and S. J. Savory, "Experimental comparison of nonlinear compensation in long-haul PDM-QPSK transmission at 42.7 and 85.4 Gb/s," in *Proc. ECOC'09*, Paper 9.4.4.
[25] H. Sun, K.-T. Wu, and K. Roberts, "Real-time measurements of a 40 Gb/s coherent system," *Opt. Exp.*, vol. 16, pp. 873–879, 2008.
[26] ITU-T Recommendation G.975.1 2004, Appendix I.9.
[27] X. Liu, S. Chandrasekhar, B. Zhu, P. J. Winzer, and D. W. Peckham, "7×224-Gb/s WDM transmission of reduced-guard-interval CO-OFDM with 16-QAM subcarrier modulation on a 50-GHz Grid over 2000 km of ULAF and five ROADM passes," presented at the ECOC'10, Paper Tu.3.C.2.

Xiang Liu (M'00-SM'05) received the M.S. degree in physics from the Institute of Physics, Chinese Academy of Sciences, Beijing, China, in 1994, and the Ph.D. degree in applied physics from Cornell University, Ithaca, NY, in 2000.

He joined Bell Labs, Holmdel, NJ, as a Member of Technical Staff in 2000. Since then, he has been primarily working on technologies for high-speed optical transport systems including advanced modulation formats, fiber nonlinearity and dispersion management, self-coherent detection, and coherent optical OFDM. He has authored and coauthored over 190 journal and conference papers, and holds over 35 US patents.

S. Chandrasekhar (F'00) received the B.Sc., M.Sc., and Ph.D. degrees in physics from the University of Bombay, Bombay, India, in 1973, 1975, and 1985, respectively.

He was at the Tata Institute of Fundamental Research, Bombay, India, from 1975 to 1985 and at AT&T Bell Laboratories (later called Lucent Technologies, Bell Laboratories and more recently called Bell Labs, Alcatel-Lucent), Crawford Hill Laboratory, Holmdel, NJ, from 1986 to the present. He initially worked on compound semiconductor devices and high-speed optoelectronic integrated circuits (OEIC's). Since January 1999, he has been responsible for forward looking research in WDM Optical Networking at 40 Gb/s and 100 Gb/s. His current interests include coherent optical orthogonal frequency division multiplexed systems for high spectral efficiency transport and networking beyond 100 Gb/s, multi-carrier superchannels, and electronic digital signal processing for software-defined transponders.

He is a DMTS at Bell Labs, a member of the IEEE Photonics Society, and was an Associate Editor of IEEE PHOTONICS TECHNOLOGY LETTERS for over ten years. He has been member of the technical program committees of the IEDM, the DRC, and the OFC conferences. He holds nineteen U.S. patents. He was awarded the IEEE LEOS Engineering Achievement for 2000 and the OSA Engineering Excellence Award for 2004 for his contributions to OEICs and WDM systems research.

Benyuan Zhu, biography not available at time of publication.

P. J. Winzer, biography not available at time of publication.

Alan H. Gnauck (M'98–SM'00–F'09) joined Bell Laboratories in 1982, where he is currently a Distinguished Member of Technical Staff in the Transmission Systems and Networks Research group.

He has performed record-breaking optical transmission experiments at single-channel rates of from 2 to 200 Gb/s. He has investigated coherent detection, chromatic-dispersion compensation techniques, CATV hybrid fiber-coax architectures, wavelength-division-multiplexing (WDM) systems, and system impacts of fiber nonlinearities. His WDM transmission experiments include the first demonstration of terabit transmission. More recently, he has demonstrated 25-Tb/s transmission. He is presently involved in the study of WDM systems with single-channel rates of 100 Gb/s and higher, using various modulation formats. He has authored or co-authored over 180 journal and conference papers, and holds 23 patents in optical communications.

Mr. Gnauck is a Fellow of the Optical Society of America (OSA) and former Associate Editor for IEEE PHOTONICS TECHNOLOGY LETTERS (2000–2009).

David W. Peckham (M'79–SM'04) received the B.S. and M.E. degrees in electrical engineering from the University of Florida, Gainesville.

He started his career at the Bell Labs Transmission Media Laboratory in 1982 working on optical fiber measurement techniques. Since 1989 he has focused on the design, process development and commercialization of optical fibers for high capacity transmission systems at Bell Labs, Holmdel, NJ, Lucent and currently OFS. He is currently a Consulting Member of Technical Staff/Research Fellow in the Optical Fiber Design Group at OFS in Norcross, GA.

Dr. Peckham received the 2002 OSA Engineering Excellence Award recognizing his contributions in the design and commercialization of fibers enabling high speed, wideband WDM networks.